Front. Med. 2019, 13(6): 690–704
https://doi.org/10.1007/s11684-018-0638-8

RESEARCH ARTICLE

Tprn is essential for the integrity of stereociliary rootlet in cochlear hair cells in mice

Yuqin Men[1], Xiujuan Li[2], Hailong Tu[1], Aizhen Zhang[1], Xiaolong Fu[1], Zhishuo Wang[1], Yecheng Jin[1], Congzhe Hou[3], Tingting Zhang[1], Sen Zhang[1], Yichen Zhou[1], Boqin Li[4,5], Jianfeng Li[6], Xiaoyang Sun (✉)[1,*], Haibo Wang (✉)[6,*], Jiangang Gao (✉)[1,*]

[1]*School of Life Science, Shandong University, Jinan 250100, China;* [2]*Rizhao Polytechnic, Rizhao 276826, China;* [3]*The Second Hospital of Shandong University, Jinan 250033, China;* [4]*Electron Microscopy Laboratory, Shandong Institute of Otolaryngology, Jinan 250022, China;* [5]*Laboratory of Electron Microscopy, Jinan WEI-YA Biotech Company, Jinan 250100, China;* [6]*Department of Otolaryngology-Head and Neck Surgery, Provincial Hospital Affiliated to Shandong University, Jinan 250021, China*

Abstract ***Tprn*** **encodes the taperin protein, which is concentrated in the tapered region of hair cell stereocilia in the inner ear. In humans,** ***TPRN*** **mutations cause autosomal recessive nonsyndromic deafness (DFNB79) by an unknown mechanism. To determine the role of** ***Tprn*** **in hearing, we generated** ***Tprn*****-null mice by clustered regularly interspaced short palindromic repeat/Cas9 genome-editing technology from a CBA/CaJ background. We observed significant hearing loss and progressive degeneration of stereocilia in the outer hair cells of** ***Tprn*****-null mice starting from postnatal day 30. Transmission electron microscopy images of stereociliary bundles in the mutant mice showed some stereociliary rootlets with curved shafts. The central cores of the stereociliary rootlets possessed hollow structures with surrounding loose peripheral dense rings. Radixin, a protein expressed at stereocilia tapering, was abnormally dispersed along the stereocilia shafts in** ***Tprn*****-null mice. The expression levels of radixin and β-actin significantly decreased. We propose that** ***Tprn*** **is critical to the retention of the integrity of the stereociliary rootlet. Loss of** ***Tprn*** **in** ***Tprn*****-null mice caused the disruption of the stereociliary rootlet, which resulted in damage to stereociliary bundles and hearing impairments. The generated** ***Tprn*****-null mice are ideal models of human hereditary deafness DFNB79.**

Keywords TPRN; stereocilia; stereociliary rootlet; actin filament; CRISPR/Cas9; hearing

Introduction

In the mammalian auditory system, an important component of the cochlea in the inner ear is the organ of Corti, which contains a single row of inner hair cells (IHCs) and three rows of outer hair cells (OHCs) [1]. Located on the apical surface of cochlear hair cells is a bundle of stereocilia that display a V-shaped staircase pattern and a uniform orientation. Stereociliary bundles are critical mechanotransducers in the hearing process. In hair cells in the inner ear, stereocilia are filled cores that consist of hundreds of actin filaments and actin-related proteins. The actin filaments and actin-related proteins are tightly packed in the basal tapered regions of the stereocilia and form electron-dense structures known as stereociliary rootlets (Fig. 1A). In mice, these stereociliary rootlets develop in the early postnatal stages. Stereociliary rootlets span roughly the entire tapered region and anchor the stereocilia in the actin-rich meshwork of the cuticular plate. The stereociliary rootlets form a durable and rigid structure to maintain the hair bundle architecture. Stereociliary bundles can pivot around the stereociliary rootlets on the surface of cochlear hair cells [2–4], and the tapered regions of stereocilia are critical hair cell structures for stereociliary deflection [5,6]. In addition to actin-based cytoskeletal structures, the actin-binding proteins in the hair cell stereocilia are necessary to maintain the steady structures

Received August 19, 2017; accepted January 27, 2018
Correspondence: Xiaoyang Sun, sunxy70@sdu.edu.cn;
Haibo Wang, wang.hb7585@hotmail.com;
Jiangang Gao, jggao@sdu.edu.cn

*Xiaoyang Sun, Haibo Wang, and Jiangang Gao contributed equally to this study.

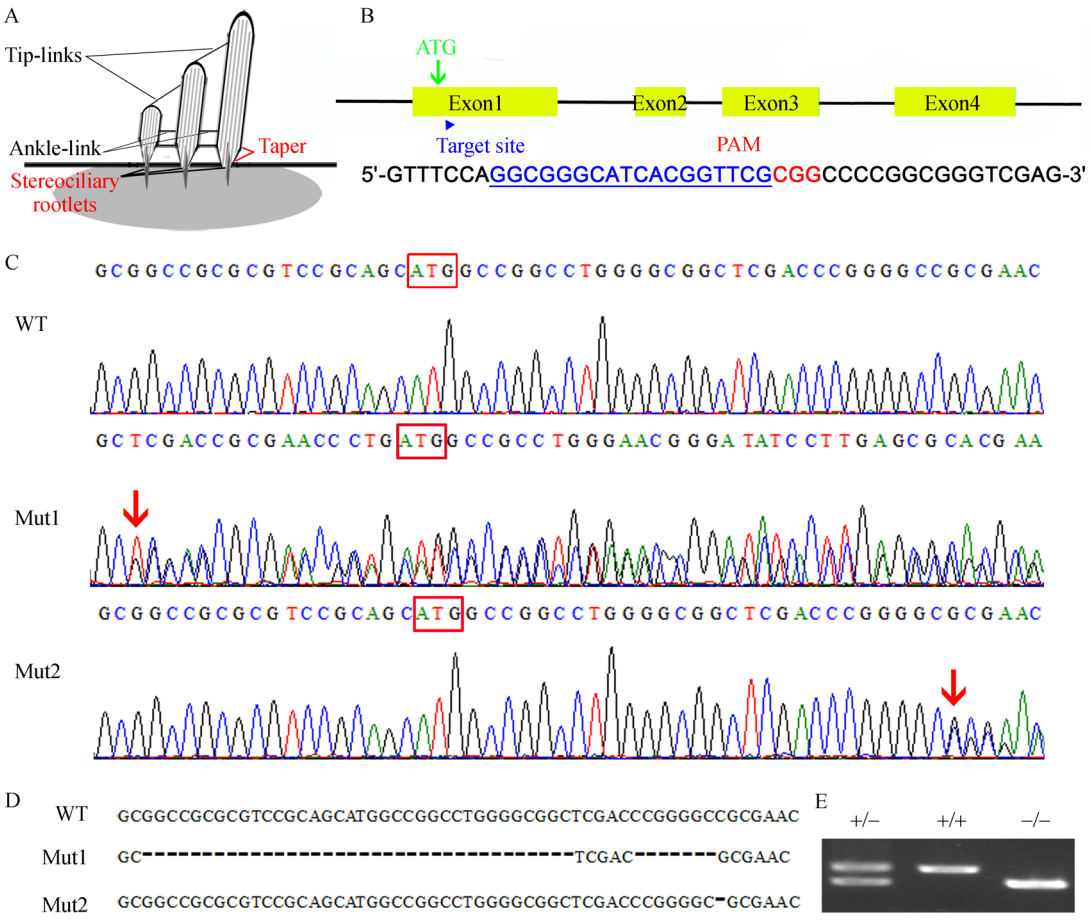

Fig. 1 CRISPR/Cas9-mediated generation of *Tprn*-null mice. (A) Diagram of stereociliary bundles in cochlear hair cells. The core of the stereocilia is composed of actin filaments. A tapered structure is located in the basal region of the stereocilia near the insertion site on the apical surface of the hair cell. (B) Schematic of the strategy. The target site (blue arrowhead) is located in exon 1 after the initiation codon ATG (green arrow). Red represents the protospacer adjacent motif (PAM) sequence. (C) DNA sequencing of the PCR products from WT and *Tprn* mutant mice at F0. The sequencing chromatograms show two mutation types. The red boxed area represents the initiation codon ATG. Red arrows signify the start sites of the mutations in mutants 1 and 2. (D) Sequences of the two mutation types (43- and 1-bp deletions). Both mutations can cause a frameshift in the *Tprn* gene. (E) Mouse genotyping by PCR analysis of *Tprn*-null mice (43-bp deletion). Lanes: heterozygous (+/–), WT (+/+), and homozygous mice (–/–). The PCR products of the WT allele was 443 bp long, the PCR products of the heterozygous *Tprn* null alleles were 400 and 443 bp long, and the PCR product of the homozygous *Tprn* null allele was 400 bp long.

of the stereociliary bundles. Previous studies reported that stereocilia often deteriorate because of mutations in proteins localized to the tapered region of stereociliary bundles; these proteins include taperin, myosin VI, radixin, protein tyrosine phosphatase receptor Q, and chloride intracellular channel 5 (CLIC5) [7–12].

TPRN encodes the taperin protein, which is expressed in many tissues, including cochlea. In mouse cochlea, TPRN is localized predominantly in the tapered regions of stereocilia in hair cells [13]. *Tprn* includes four exons that encode a protein of 711 amino acids [14]. In humans, mutations in *TPRN* are associated with human deafness DFNB79 in several families, such as consanguineous Pakistani and Moroccan families [13,14]. All of the deafness-associated *TPRN* mutations are located in exon 1. The exon 1 of *TPRN* is a hotspot for mutations because of the presence of elements that contain high numbers of GC-rich repeats [13]. The existence of deafness-associated mutations in *TPRN* in humans demonstrates that *TPRN* plays a critical function in hearing. TPRN forms a protein complex with radixin, myosin VI, and CLIC5 to stabilize membrane actin filament linkages [15]. Furthermore, TPRN localization is perturbed in the absence of the deafness gene *Fam65b*, which is critical to the maintenance of the structural organization of the basal domain of stereocilia. This finding indicates that the functions of *Fam65b* and *Tprn* are interdependent [16]. Thus, *Tprn* is closely associated with deafness genes, such as *Radixin*, *Clic5*, and *Fam65b*.

In a previous study, TPRN-deficient mice from a

C57BL/6 background were generated through transcription activator-like effector nuclease (TALEN) technique [17]. The mice showed progressive hearing loss and had degenerated hair cell stereocilia. The study failed to address the following issues: (1) TPRN is an important component of stereociliary rootlets in cochlear hair cells, and its function in the stereociliary rootlets needs to be examined; and (2) the mechanism by which TPRN deficiency results in phenotypes remains to be elucidated. Moreover, the C57BL/6 mouse strain as a mouse model is unsuitable to hearing research. The C57BL/6 mouse strain [wild type (WT)] suffers from age-related hearing loss (ARHL) [18]. In the present study, we applied clustered regularly interspaced short palindromic repeat (CRISPR)/Cas9-mediated genome-editing technology to delete TPRN from CBA/CaJ mice, which are considered the best strain for hearing-related research [18]. Therefore, *Tprn*-null mice with the CBA/CaJ background are ideal models of nonsyndromic deafness DFNB79 for hearing research. In addition to progressive stereocilium degeneration, defects in stereociliary rootlets were evident in *Tprn*-null mice. These defects could be due to the failure of the interaction between radixin and TPRN. These findings suggest that TPRN plays an essential role in normal hearing by maintaining intact stereociliary rootlets in mice and that the defected stereociliary rootlets cause hair cell stereocilium degeneration and hearing loss.

Materials and methods

Ethics statement

Tprn-null mice were generated in the animal facility of the School of Life Science at Shandong University. All animal experimental procedures and management were performed strictly in accordance with the guidelines of the Animal Ethics of Shandong University.

Generation of *Tprn* knockout mice

Tprn-null mice were generated through the CRISPR/Cas9 genome-editing technology on the background of the CBA/CaJ mouse line. CRISPR/Cas9 genome-editing technology in mice was performed as previously described in detail [19]. A pX330 plasmid (Plasmid ID: #42230) was obtained from Addgene. The pX330 plasmid contained humanized Cas9 (hCas9) under the chicken hybrid promoter and multiple cloning sites into which oligos for sgRNA could be inserted. A pair of sgRNA target oligonucleotides (5′-GGGCCGCGAACCGTGATGCC-3′) were annealed and inserted into the multiple cloning sites of the pX330 vector. sgRNA was under the human U6 promoter in the vector. The pX330 vector that contained hCas9 and sgRNA was purified using a MEGAclear kit (Ambion).

CBA/CaJ female mice were superovulated and mated with CBA/CaJ males. Fertilized eggs were isolated from the oviducts of the female mice the next morning. The purified circular pX330 vector was microinjected into the pronucleus of fertilized eggs under an inverted microscope. The injected fertilized eggs were incubated in KSOM-AA medium (Millipore) for 10 min and transferred into the oviducts of pseudopregnant CD1 female mice. The mutated gene in the resulting mice was identified by extracting genomic DNA from the tails of pups, and a DNA fragment that surrounded the target site in the *Tprn* exon 1 was amplified through polymerase chain reaction (PCR). The PCR products were subjected to sequencing or cloned using T/A cloning method and sequenced. PCR was performed using the following primers: *Tprn* forward primer 5'-ACCTCGTGCTTGTTCAG-3' and *Tprn* reverse primer 5'-TGTCTTCAGCAGGGTGT-3'.

Analysis of potential off-target mutations

The potential off-target site sequences of sgRNA were predicted using CRISPR DESIGN (http://crispr.mit.edu/). One potential off-target site for *Tprn* was found, and primers for off-target analysis were designed as follows: *Cdc45* forward: 5′-TTCGGGCGGAAGTAATC-3′ and *Cdc45* reverse: 5′- ACTCCTTGCGGAAATCG-3′.

Genomic DNA fragments from pups were amplified by PCR by using the primers listed above. The PCR products were sequenced directly or cloned using T/A cloning method and sequenced to identify the mutations of off-target sites.

Genotyping

WT, heterozygous *Tprn*-null, and homozygous *Tprn*-null mice were genotyped by PCR of genomic DNA extracted from mouse tail snips. The mice were genotyped with the same primers to identify the mutations described above. The genotyping results were evaluated on the basis of the PCR product size to delete large DNA fragments. For short deletion mutations, the genotyping results were determined by PCR product sequencing.

Auditory brainstem response (ABR)

The ABRs of WT, heterozygous *Tprn*-null, and homozygous of *Tprn*-null mice aged 1 month to 6 months were recorded. ABR tests were performed as described previously [20]. In brief, the mice were anesthetized with 0.007 g/mL sodium pentobarbital and placed in a soundproof room. All ABR recordings were captured by three subdermal needle electrodes. The positive electrodes were placed at the midline vertex, the negative electrode over the mastoid of the right ear, and the ground electrode on the rear region above the tail. ABR tone pips at frequencies of

4, 8, 16, and 32 kHz were generated using a Tucker–Davis Technologies workstation that ran SigGen32 software. The auditory thresholds of ABR at the broadband click and pure tone were determined by decreasing the sound intensity from 90 dB to 10 dB until the lowest response waveform could no longer be identified.

Statistical comparison of the mean was performed by Student's *t*-test with Bonferroni correction. About $n > 4$ animals per genotype were used. Mean values are shown as ± standard error around the mean, and $P < 0.05$ indicates statistically significant difference.

Whole-mount immunostaining

Whole-mount immunostaining was performed as described previously [21]. Cochleae from the WT and *Tprn*-null mice were dissected, fixed in 4% paraformaldehyde (PFA) for 2 h at room temperature, and decalcified in 10% ethylene diamine tetraacetic acid (EDTA) overnight at 4 °C. In the morning of the following day, the cochleae were dissected into three sections, namely, the apical, middle, and basal turns of the basilar membrane. The samples were washed with 10 mmol/L PBS and stained with primary antibody overnight at 4 °C. The samples were then incubated in secondary antibodies for 1 h at room temperature and washed in phosphate-buffered saline (PBS). Finally, the samples were stained with rhodamine phalloidin (Sigma) and nuclear stain 4,6-diamidino-2-phenylindole (DAPI), followed by final washing in PBS. The cochleae were visualized using an LSM 700 confocal microscope.

The primary antibodies used in this study were anti-TPRN polyclonal antibody (rabbit, Sigma), anti-myosin VIIa polyclonal antibody (rabbit, Proteus-Bioscience), anti-prestin polyclonal antibody (goat, Santa Cruz), and anti-radixin polyclonal antibody (rabbit, Abcam).

FM1-43 uptake assay

FM1-43 uptake assay was performed as previously described [22]. Briefly, cochleae were dissected from WT and *Tprn*-null mice. The cochlear samples were treated with 2 μmol/L FM1-43 dye (Invitrogen) in PBS for 20 s and fixed with 4% PFA overnight at 4 °C. The next morning, the samples were washed three times in 10 mmol/L PBS. The cochleae were observed under an LSM 780 confocal microscope.

Western blot analysis

The cochleae from the WT and *Tprn*-null mice were rapidly dissected, incubated in cell lysis buffer (10 mmol/L Tris, pH = 7.4, 1% Triton X-100, 150 mmol/L NaCl, 1 mmol/L EDTA, and 0.2 mmol/L PMSF), and extracted using a homogenizer. The protein samples (20 μg) were subjected to sodium dodecyl sulfate–polyacrylamide gel electrophoresis and blotted onto a polyvinylidene difluoride membrane. Western blot analysis was performed as described previously. The primary antibodies used in this study were anti-radixin polyclonal antibody (rabbit, Abcam), anti-glyceraldehyde-3-phosphate dehydrogenase monoclonal antibody (mouse, Millipore), and anti-β-actin polyclonal antibody (rabbit, Bioworld).

Scanning electron microscopy (SEM)

Under sodium pentobarbital anesthesia, WT and *Tprn*-null mice were transcardially perfused with 4% PFA. The temporal bone cochleae were dissected and immersed in 2.5% glutaraldehyde overnight at 4 °C. The next morning, the cochleae were dissected, post-fixed in 1% osmium tetroxide for 1 h, and washed in ddH_2O. The samples were dehydrated through a graded ethanol series, critically point dried, mounted, and sputter coated with gold. The stereociliary bundles of the cochleae were examined in a Hitachi S-4800 field-emission scanning electron microscope.

Transmission electron microscopy (TEM)

TEM analysis was performed as previously described [23]. Cochleae from WT and *Tprn*-null mice were dissected rapidly and pierced with a pole at the apex. The cochleae were fixed from the pierced pole at the apex, immersed in 2.5% glutaraldehyde overnight at 4 °C, and post-fixed with 1% osmium tetroxide. Images were acquired using a JEOL-1200 electron microscope.

Statistical analysis

All Western blot data are presented as mean ± standard error around the mean, and significance was determined by Student's *t*-test by using ImageJ and GraphPad Prism 5.0 software. The significance level was set to $P < 0.05$ for all statistical analyses. Quantitative analyses of the stereocilium degeneration and diameter measurements of the tapered region were performed. All data are presented as mean ± standard error around the mean, and significance was determined by Student's *t*-test through the GraphPad Prism 5.0 software. The significance level was set to $P < 0.05$ for all statistical analyses.

Results

CRISPR/Cas9-mediated generation of *Tprn*-null mice

We performed CRISPR/Cas9-mediated genome editing to delete the *Tprn* gene from the background of the CBA/CaJ mouse strain. An sgRNA target in exon 1 of the *Tprn* gene

was selected immediately after the initiation codon (ATG, Fig. 1B). The pX330 vector containing hCas9 and sgRNA was injected into zygotes by pronuclear microinjection to generate *Tprn*-null mice. Eighteen days after transplantation, seven pups were born and designated as F0. Among them, two F0 mutant founders were identified. The PCR products from these two F0 mutant mice were cloned through the T/A cloning method and sequenced. One founder was found to include one frame shift mutation (–1 bp). The second founder contained a 43-bp deletion in one chromosome and a 15-bp deletion in the other chromosome. The F1 *Tprn* heterozygous mutant mice, which harbored the 1- or 43-bp deletion, were obtained by breeding the F0 mice with the WT CBA/CaJ mice (Fig. 1C). The two mutants with 1- or 43-bp deletion were selected as our research subjects because they caused a frame shift in the *Tprn* gene (Fig. 1C). The F1 heterozygous mice were inbred for one generation, and homozygous strains were obtained for each of the mutations in the *Tprn* gene. The two homozygous strains of *Tprn*-null mice, one with a 1-bp deletion and another with a 43-bp deletion, were examined by sequencing (Fig. 1D) or PCR (Fig. 1E). The two homozygous strains of *Tprn*-null mice exhibited the same phenotype in the inner ear hair cells. Off-target effects are a hallmark of CRISPR/Cas9 technology; therefore, we analyzed the potential off-target site sequences of the sgRNA as predicted using CRISPR DESIGN (http://crispr.mit.edu/). We found no off-target mutations in this analysis of the *Tprn* mutant mice.

The *Tprn*-null mice exhibited no obvious defect in gross morphology. The mice were fertile and comparable in size to the WT littermates (Fig. 2A). We dissected the temporal bones of the inner ear and observed no obvious abnormality in the cochlea of the *Tprn*-null mice (data not shown). Whole mount immunostaining was performed to examine TPRN expression in the WT and mutant mice. A high level of TPRN expression was detected around the base of the stereociliary bundle in the hair mice (Fig. 2B). By contrast, no TPRN expression was detected in the cochlear hair cells of the *Tprn*-null mice (Fig. 2B). These results indicated that we successfully generated a *Tprn*-null mouse model (*Tprn*$^{-/-}$ mice).

Hearing loss in *Tprn*-null mice

We tested the auditory brainstem responses (ABRs) of *Tprn*-deficient mice at 1, 2, 4, and 6 months of age to assess their hearing sensitivity (Fig. 3). Measuring ABRs to broadband click stimuli demonstrated that the *Tprn*-null mice exhibited progressive hearing loss with a sound pressure level (SPL) that increased from 34 dB at 1 month of age to 60 dB at 6 months of age, whereas the control mice showed normal hearing thresholds that ranged from 25 dB to 33 dB at all the ages assessed (Fig. 3A). ABR recordings in response to pure tones at different frequencies were also evaluated. In the 1 month-old WT mice, the ABR thresholds varied with frequency from an SPL of 55 dB at 4 kHz (relatively low frequency for mice) to 57 dB at 32 kHz (relatively high frequency; Fig. 3B). The 2, 4, and 6 month-old WT mice retained normal hearing thresholds, as assessed by the ABRs. The ABR thresholds of the 1 month-old *Tprn*-null mice were 5 dB to 15 dB higher than those of the 1 month-old WT mice (Fig. 3B). In the 2 month-old *Tprn*-null mice, the hearing thresholds were 5 dB to 20 dB higher (Fig. 3C) than those of WT mice at the same age. The ABR thresholds in the 4 month-old *Tprn*-null mice were 10 dB to 25 dB higher than those in the 4

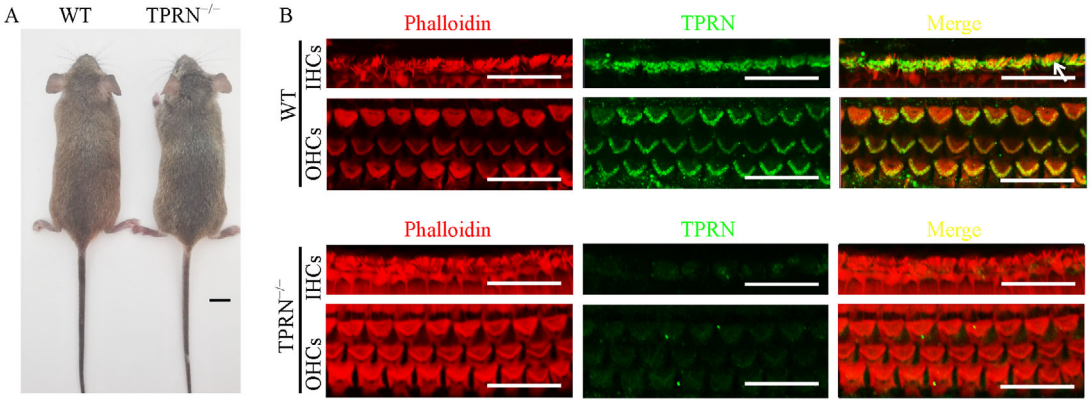

Fig. 2 Expression pattern of TPRN in cochlear hair cells of WT mice. (A) Gross morphology of P21 WT and *Tprn*-null mice. No obvious difference, including that in the body size, was noted. Scale bar: 1 cm. (B) Confocal images of cochlear hair cells stained with anti-taperin antibody in P30 WT and *Tprn*-null mice. TPRN was enriched at the basal tapered region of stereociliary bundles in cochlear hair cells (arrows) in the WT mice. Taperin expression was not detected in the cochlear hair cells of *Tprn*-null mice. The inserts represent high-magnification views of the boxed areas. Red, phalloidin; green, TPRN. Scale bar: 20 μm.

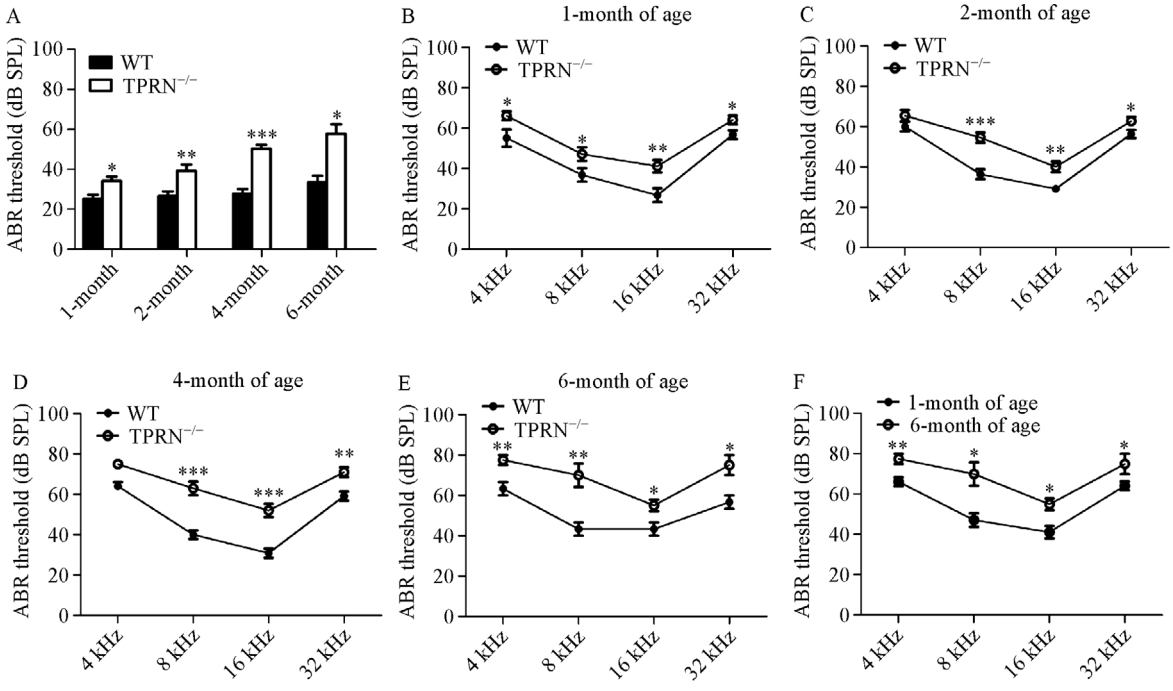

Fig. 3 ABR test in WT and *Tprn*-null mice at different ages. (A) ABR measurements for broadband click in the 1, 2, 4, and 6 month-old mice. (B–E) ABR measurements for frequency-specific pure tone stimulation in the 1, 2, 4, and 6 month-old mice. (F) Hearing thresholds by ABR testing for frequency-specific pure tone stimulation in *Tprn*-null mice at 1 and 6 months of age. The data indicated a progressive elevation of thresholds from 1 month to 6 months of age. * $P < 0.05$; ** $P < 0.01$; *** $P < 0.001$ compared with the WT thresholds at the corresponding frequency as determined by Student's *t*-test; $n > 4$.

month-old WT mice (Fig. 3D). By 6 months of age, the *Tprn*-null mice showed 15 dB to 30 dB higher hearing thresholds across almost all frequencies tested than those of WT mice (Fig. 3E). Deletion of TPRN resulted in a significant elevation in hearing threshold compared with that of WT mice. From 1 month to 6 months of age, the *Tprn*-null mice showed a gradual increase in hearing thresholds (Fig. 3F), which indicated progressive hearing loss in the mutant mice.

Progressive degeneration of stereocilia of inner ear hair cells and occasional loss of hair cells in *Tprn*-null mice

We examined the morphology of stereociliary bundles and the cuticular plate in the hair cells of the mice using cochlear whole mounts stained with phalloidin. No obvious defect was observed in the stereociliary bundles and cuticular plate in the *Tprn*-null mice at the age of 1 month (Fig. 4A). We stained for DAPI and hair-cell-specific markers, including myosin VIIa and prestin, to visualize hair cell nuclei, hair cell bodies, and hair cell lateral membranes. The results showed that the morphology of the cochlear hair cells of the *Tprn*-null mice was normal compared with that of WT mice (Fig. 4A). At the age of 4 months of the mice, the cochlear whole-mount staining images showed no other obvious defect except that observed in the morphology of stereociliary bundles (Fig. 4B and 4C). High-magnification images showed an evident loss of stereocilia in the *Tprn*-null hair cells (Fig. 4C, arrowheads). Occasional OHC loss was also found in the basal turn of the 4 month-old *Tprn*-null mice. The *Tprn*-null mice suffered from evident loss of OHCs at the age of 6 months (Fig. 4D).

The morphologies of the stereociliary bundles in cochlear hair cells were examined through SEM. A minor disorder in stereociliary bundles and no hair cell loss were observed in the IHCs of the *Tprn*-null mice (Fig. 5). High-resolution SEM images of OHCs showed a minimal loss of stereocilia from the innermost stereocilia row in the 1 month-old *Tprn*-null mice (Fig. 5A, white arrows). The rates of degeneration and loss of stereocilia in the OHCs of the 2 month-old mutant mice were higher than those in the OHCs of the 1 month-old mice (Fig. 5B, white arrows). In the 4 month-old *Tprn*-null mice, the stereocilium degeneration and loss in the OHCs aggravated (Fig. 5C, white arrows). The remaining stereociliary bundles in the *Tprn*-null mice were quantitatively analyzed, and the results demonstrated that 95% of the bundles were retained at 1 month of age and 74% at 4 months of age. Accordingly, the progressive degeneration and loss of stereocilia started to occur in the OHCs of the *Tprn*-null mice at 1 month of age. Apart from the

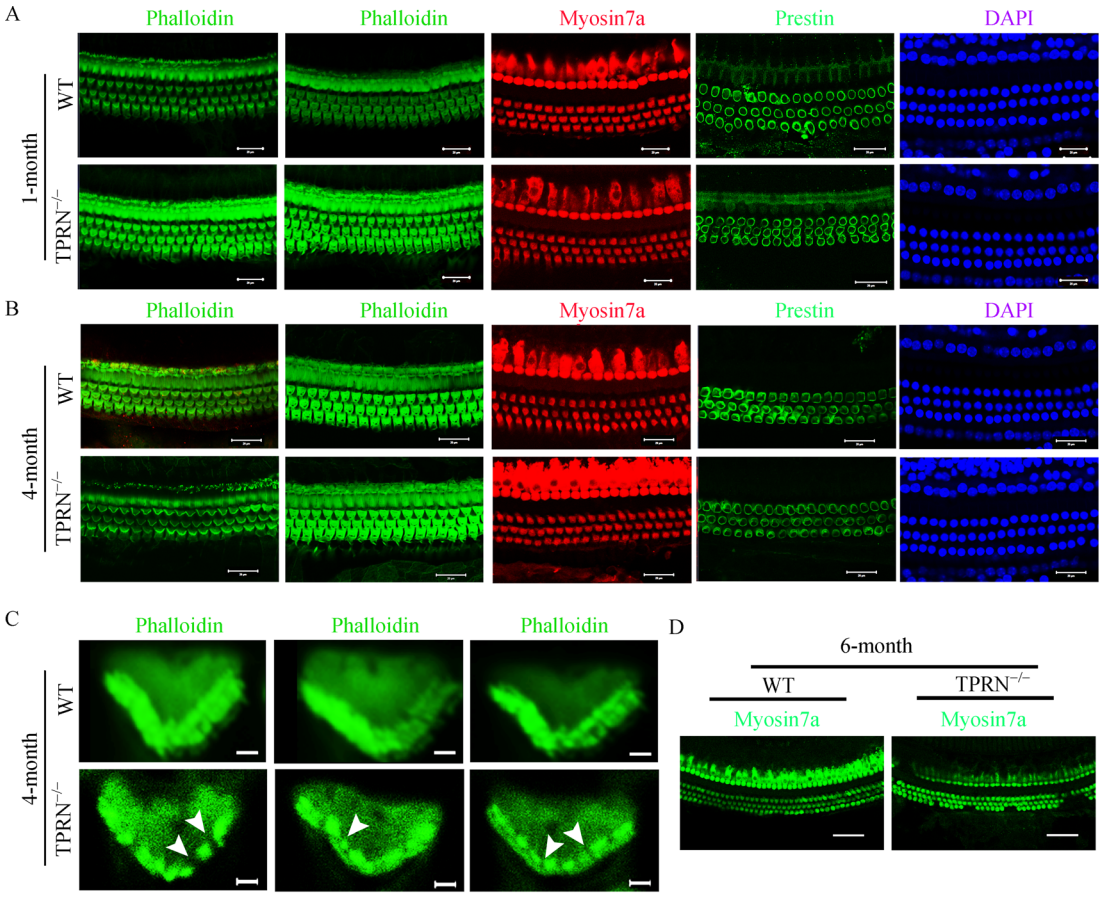

Fig. 4 Immunostaining of whole-mount cochleae from WT and *Tprn*-null mice. (A) Confocal images of hair cells stained with the F-actin dye phalloidin, the hair cell marker myosin VIIa (red), the OHC lateral membrane marker prestin (green), and the cell-nucleus-specific dye DAPI (blue) in 1 month-old mice. No obvious defect was found in the hair cells of the *Tprn*-null mice. Scale bars: 20 μm. (B) Confocal images of hair cells stained with phalloidin, myosin VIIa (red), prestin (green), and DAPI (blue) in 4 month-old mice. The morphology of the hair cells appears normal. Scale bars: 20 μm. (C) High-magnification images of stereociliary bundles show evident gaps in the stereociliary bundle and indicate a loss of stereocilia in the 4 month-old *Tprn*-null mice (arrowheads). Scale bars: 20 μm. (D) Confocal images of hair cells stained with myosin VIIa (green) in 6 month-old mice. A severe hair cell loss was observed in the basal turn of cochlea in *Tprn*-null mice. Scale bars: 50 μm.

degeneration of the shortest stereocilia of the OHCs, occasional missing OHCs were detected in the basal turns of the cochlea in the 4 month-old mice (Fig. 5).

Given the localization pattern of TPRN among the hair cells, we closely observed the structural changes near the stereocilia base. In the SEM images, thinner stereocilia were found in the mutant mice than those in the WT mice, especially in the tapered region (Fig. 6A, arrowheads). The diameters of the tapered region in the stereociliary bundles were measured in WT and *Tprn*-null mice. No significant change in stereocilia diameter was observed in the *Tprn*-null mice relative to that in the WT mice before postnatal day 14 (Fig. 6A and 6A′). Significantly thin diameters of stereocilia were found in the *Tprn*-null mice starting from postnatal day 30 with respect to those of the WT mice (Fig. 6A and 6A′). High-magnification images of stereociliary bundles in the red boxed areas show evident gaps in the *Tprn*-null mice at P120 (Fig. 6A and 6A′).

Abnormal stereociliary rootlets of cochlear hair cells in the *Tprn*-null mice

The structure of stereociliary rootlets at the tapered region of stereociliary bundles was examined by TEM. In the vertical ultrathin sections of hair cells from the WT mice, the stereociliary rootlets of all three rows appeared straight among the stereociliary bundles of the tapered region (Fig. 7A, white arrowheads). However, some stereociliary rootlets in the *Tprn*-null mice exhibited curved shafts (Fig. 7A, black arrowheads) compared with those of the WT mice.

In the horizontal sections of the hair cells, we observed a densely packed central core of stereociliary rootlets (Fig. 7B, yellow arrowheads) surrounded by a peripheral-dense ring in the WT mice (Fig. 7B, white arrowheads). A uniform alignment of stereociliary rootlets with a dot-like shape (Fig. 7C, yellow arrowheads) at the cuticular plate

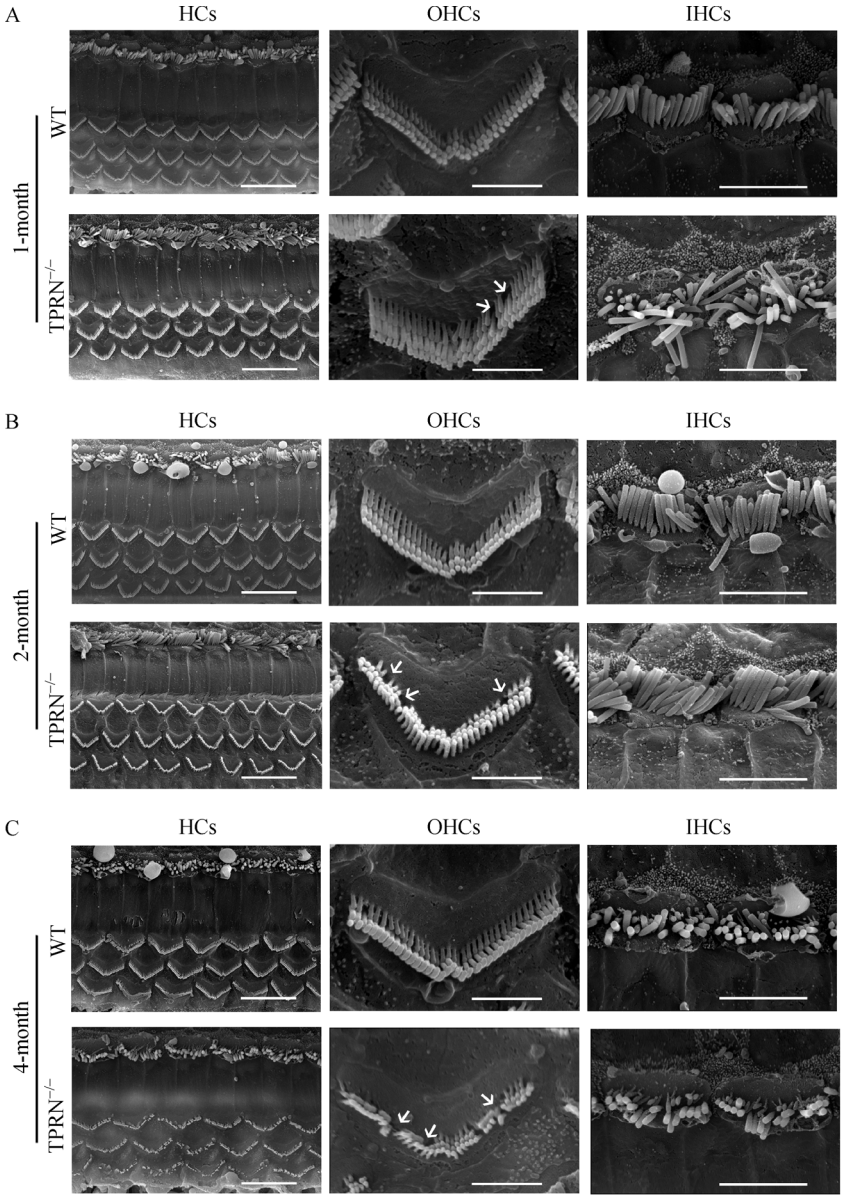

Fig. 5 SEM images of stereocilia in *Tprn*-null mice. (A) Images of hair cell bundles in the WT and *Tprn*-null mice at 1 month of age. (B) Images of hair cell bundles in the WT and *Tprn*-null mice at 2 months of age. (C) Images of hair cell bundles in the WT and *Tprn*-null mice at 4 months of age. Scale bars: 10 μm for HCs; 2 μm for OHCs; 5 μm for IHCs.

was also noted in the arms of the V-shaped stereociliary bundles (Fig. 7C, black arrows) in the WT mice. By contrast, the stereociliary rootlets of the *Tprn*-null mice were not aligned and showed a disorganized arrangement (Fig. 7C, black arrows). These results were consistent with the observation that mutant mice possessed curved stereociliary rootlets in the vertical sections of stereocilia (Fig. 7A, white arrowheads). An evident hollow structure was persistently observed in the central cores of the stereociliary rootlets of the *Tprn*-null mice (Fig. 7C, yellow arrowheads) but not in the WT mice. The central core was less compact and the peripheral-dense ring around the stereociliary rootlet was looser (Fig. 7B, white arrowheads) in the *Tprn*-null mice than in the WT mice.

Mechanotransduction defects of the stereocilia of cochlear hair cells in *Tprn*-null mice

The stereocilia in cochlear hair cells are critical mechanotransducers during hearing onset. *Tprn* expression is highly concentrated at the tapered region of stereociliary bundles. In our study, given the severely disrupted structure of stereociliary rootlets at the tapered region of the stereociliary bundles, we performed an experiment to

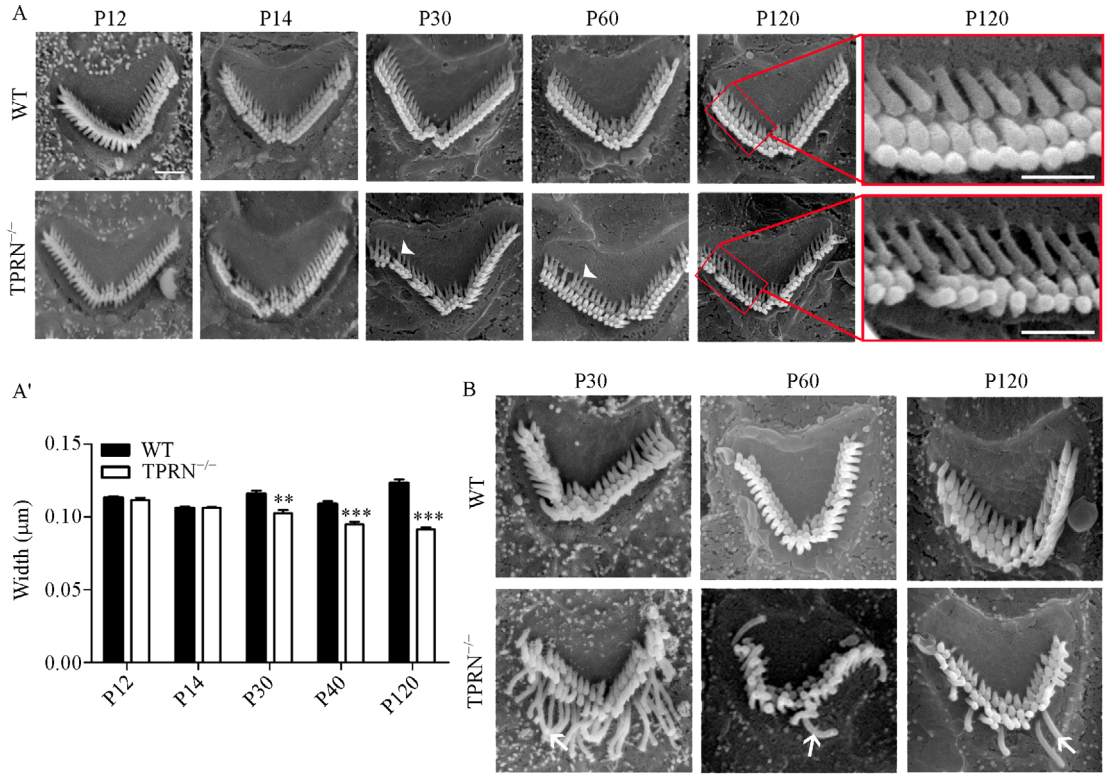

Fig. 6 Defects in the tapered region of stereocilia and some elongated stereocilia in *Tprn*-null mice. (A) SEM images of stereocilia in mice at P12, P14, P30, P60, and P120. The diameters of the tapered region in the stereocilia were thinner in the *Tprn*-null mice than in the WT mice, starting from 1 month of age. Red inserts represent a high-magnification view of the red boxed areas. Highly magnified images of stereociliary bundles show evident gaps in the stereocilia of *Tprn*-null mice at P120. Scale bar: 5 μm. (A′) Statistical analysis of the diameters of the tapered region in the innermost row of stereocilia. OHCs were selected in the same region at the midbasal turn of the cochlea, and the diameters of the tapered region in the stereocilia were measured. Data are shown as the mean ± standard error around the mean. Significance was calculated by Student's *t*-test. *$P < 0.05$; ** $P < 0.01$; *** $P < 0.001$; $n > 10$. (B) SEM images of stereocilia at the apical turn of the cochlear OHCs at the ages of 1, 2, and 4 months.

determine whether defects in mechanotransduction exist in mutant hair cells. In particular, an assay for FM1-43 uptake was performed in the hair cells of the WT and *Tprn*-null mice (Fig. 8). FM1-43 is a fluorescent dye that can be assimilated through the mechanotransduction channels of hair cells. We observed high levels of FM1-43 uptake in the WT hair cells, but very low levels of FM1-43 uptake in the *Tprn*-null hair cells in mice at 4 months of age (Fig. 8). These data indicated the presence of an evident defect in the functioning of stereociliary bundles in the *Tprn*-null mice.

Abnormal distribution of radixin and decreased expression of radixin and β-actin in *Tprn*-null mice

The cytoskeletal core of stereociliary bundles is composed of an actin filament core and actin-binding proteins, such as radixin [24], villin [25], fimbrin [26], XIRP2 [27], and FASCIN2 [28]. The actin filament core of stereocilia at the basal tapered region is tightly packed into electron-dense rod-like structures (stereociliary rootlets). TPRN has been reported to be highly expressed in the tapered regions of stereocilia, especially the core stereociliary rootlets, and taperin interacts with radixin in the tapered domain of the stereocilia [15]. Therefore, we focused on the actin-binding protein radixin. Radixin expression was examined by immunostaining with anti-radixin antibody. In the hair cells of the WT mice, radixin was enriched at the stereocilium base, with very low levels in the shaft of the stereociliary bundles (Fig. 9A). However, in the *Tprn*-null hair cells, radixin was expressed diffusely throughout the stereocilia (Fig. 9B). We then examined the level of radixin by Western blot. The results showed that the expression level of radixin in the *Tprn*-null mice was significantly lower than that in the WT mice (Fig. 9C). In addition, we examined the expression level of β-actin, a critical component of actin filaments, by Western blot. The β-actin amount was significantly decreased in the *Tprn*-null mice with respect to that in the WT mice (Fig. 9D). These results suggested that TPRN deficiency in the *Tprn*-null

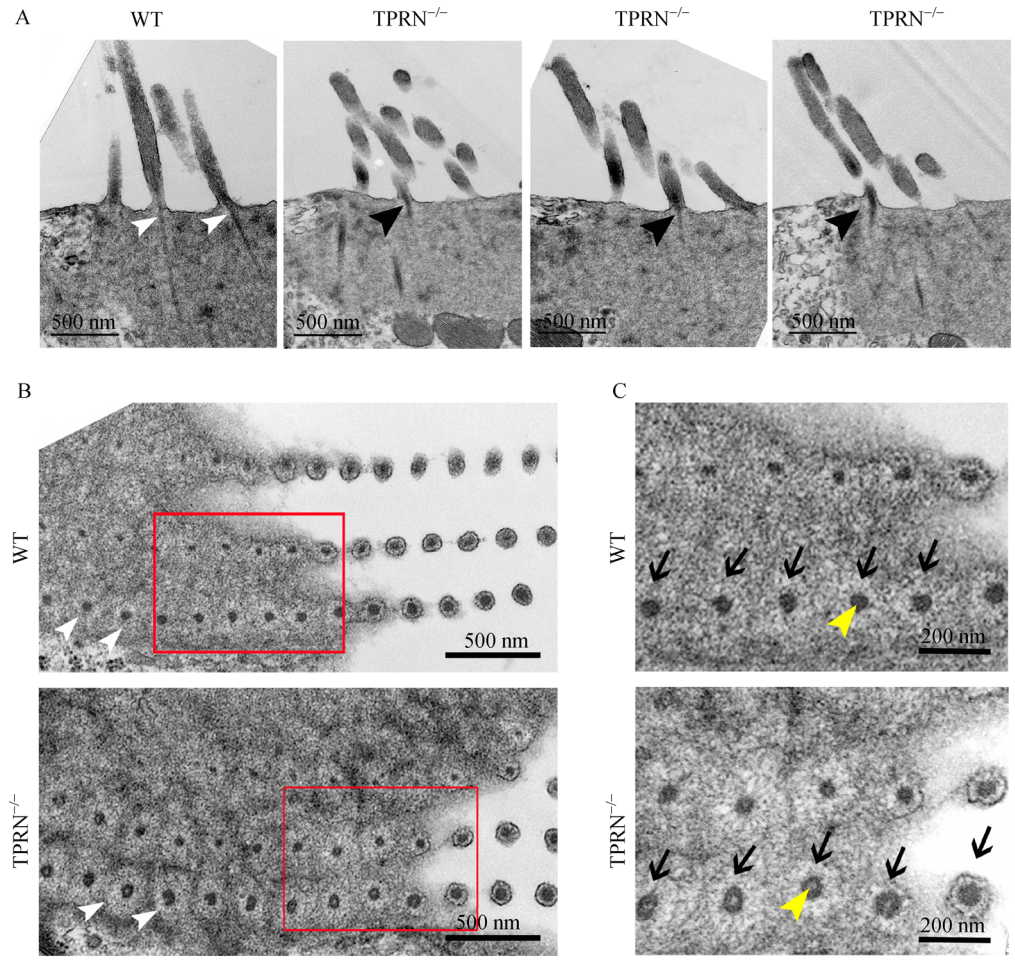

Fig. 7 Disrupted structure of stereociliary rootlets in *Tprn*-null mice. (A) TEM images of the vertical ultrathin sections of hair cells at the middle–basal turns of the cochlea in the 2 month-old mice. In the WT mice, the stereociliary rootlets of the stereocilia were straight (white arrowheads) and penetrating into the cuticular plate. By contrast, the stereociliary rootlets curved (black arrowheads) in the *Tprn*-null mice. Scale bars: 500 nm. (B) TEM images of the horizontal sections of stereociliary bundles in the 2 month-old mice. In the WT hair cells, an electron-dense central core and a peripheral-dense ring around the stereociliary rootlets were observed at the stereocilium base (white arrowheads). In the *Tprn*-null mice, a loose peripheral ring was observed surrounding the core actin structure (white arrowheads) but not in the WT mice. Scale bars: 500 nm. (C) High-magnification view of the red boxed areas in Fig.7B. In the WT hair cells, horizontal sections showed a uniformly aligned electron-dense central core (yellow arrowheads and black arrows) on the apical surface of cochlear hair cells. In the *Tprn*-null mice, the core of stereociliary rootlets shows an evident hollow structure (yellow arrowheads). The stereociliary rootlets in the three rows were arranged disorderly (black arrows). Scale bar: 200 nm.

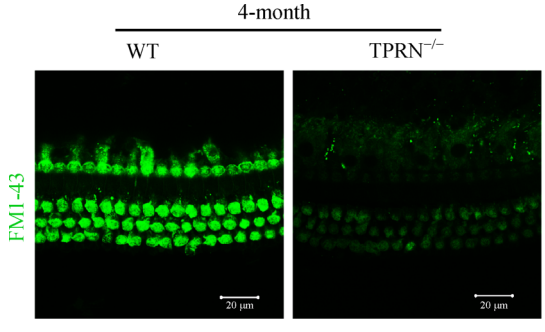

Fig. 8 Analysis of mechanotransduction channels in the hair cells of *Tprn*-null mice. FM1-43 uptake assay in the hair cells of WT and *Tprn*-null mice at 4 months of age. The FM1-43 assay in the WT mice displayed high FM1-43 uptake, whereas the *Tprn*-null hair cells exhibited very low FM1-43 uptake.

mice affected the distribution of radixin, decreased the expression levels of radixin and β-actin, and disrupted the actin-based stereociliary structures.

Discussion

Previous studies have reported that mutations in *TPRN* cause progressive autosomal recessive nonsyndromic deafness DFNB79 [13,29]. The TPRN-deficient mice established by TALEN from a C57BL/6 background show sensorineural hearing loss and degeneration [17]. However, the precise function of TPRN in the hearing process remains obscure, and the mechanisms by which TPRN deficiency causes phenotypes must be determined. In our study, for the comprehensive investigation of the

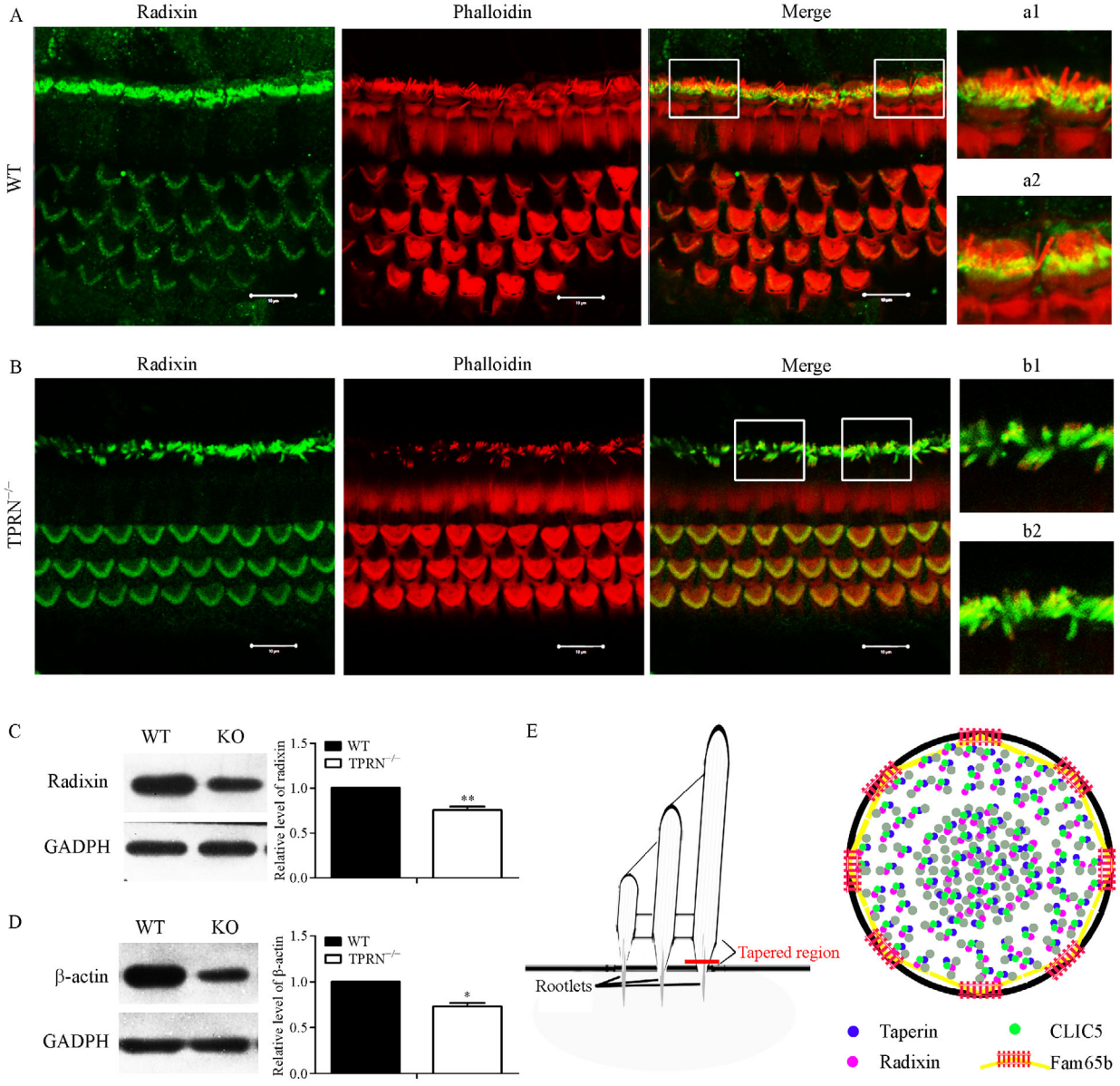

Fig. 9 Ectopic localization of radixin and decreased levels of radixin and β-actin in *Tprn*-null cochleae. (A, B) Radixin protein localization in the hair cells of 2 month-old mice. (A) In the WT mice, radixin staining was mainly detected at the base of the stereociliary bundles. (B) In the *Tprn*-null mice, radixin was diffusely distributed along the stereocilia shafts. (a1, a2; b1, b2) Boxed areas represent the high-magnification view in the WT mice (a1, a2) and *Tprn*-null mice (b1, b2). Red, phalloidin; green, radixin. Scale bars: 20 μm. (C, D) Western blot analysis of radixin (C) and β-actin (D) protein levels in the mouse cochleae at P30. (C) Radixin protein quantification indicated that the expression levels were significantly decreased in the *Tprn*-null mice. (D) β-actin protein quantification denoted that the expression levels were significantly decreased in the *Tprn*-null mice. The data were normalized against the results of the WT mice. Error bars indicate the standard error around the mean. * $P < 0.05$; ** $P < 0.01$; *** $P < 0.001$ compared with the WT mice by Student's *t*-test; $n = 3$. (E) Model of actin filament core and actin-binding proteins, including taperin, at the tapered region of stereocilia. Fam65b formed a circumferential ring-like structure at the tapered region of stereocilia. TPRN was inside the ring-like structure and formed a protein complex with CLIC5 and radixin. The TPRN-related protein complex could stabilize membrane/actin filament linkages in the cochlear stereocilia, including stereociliary rootlets. The dense structure of actin filaments in a stereociliary rootlet was critical for maintaining and stabilizing stereocilia.

function of TPRN in hearing, *Tprn*-null mice were generated through using CRISPR/Cas9-mediated genome-editing technology in CBA/CaJ mice, the best strain for hearing-related study. Significant hearing loss and

progressively degenerating stereocilia were observed in *Tprn*-null mice. Stereocilia with damaged stereociliary rootlets were found in mutant mice. An abnormal distribution of radixin and reduced expression levels of radixin and β-actin were also noted. These levels may adversely affect the maintenance and stabilization of actin filaments. We propose that TPRN is required for stabilizing hair cell stereocilia by maintaining intact stereociliary rootlets, and TPRN dysfunction can cause hearing loss in mice.

Tprn is required for the maintenance rather than the development of stereociliary bundles in cochlear hair cells in mice

In our study, the ABR threshold in the *Tprn*-null mice was significantly elevated starting at 1 month of age. Threshold elevation was highly aggravated in 6 month-old *Tprn*-null mice. These findings indicated that *Tprn* is required for normal hearing in mice and *Tprn* ablation can cause progressive hearing loss. However, a functional deficiency in hearing sensitivity often results from the structural damage of hair cells, especially the abnormal morphology of stereociliary bundles in the inner ear [30–33]. In *Tprn*-null mice, we found progressively degenerating stereocilia and thinned stereocilia diameters, especially at the tapered region. These results suggested that the malformation of stereociliary actin-based cytoskeletal structures may have contributed to the significantly elevated hearing thresholds in the *Tprn*-null mice.

The development and maturation of stereociliary bundles in mice are complex and precisely regulated processes. Cochlear stereociliary bundles continue to develop after birth until functional maturation with hearing onsets initially at around postnatal day 14 [34,35]. In this study, no obvious morphological defect in the hair cell stereociliary bundles of the *Tprn*-null mice was observed in the SEM images before postnatal day 14. Thus, the development of the stereociliary bundles in the hair cells of *Tprn*-null mice is normal. At 1 month of age, the *Tprn*-null mice began to display degenerating stereocilia, especially at the innermost row of stereociliary bundles. More severe abnormalities in the stereociliary bundles were observed in the 4-month-old mutant mice. With the progressive degeneration of stereociliary bundles, severe OHC loss was noted at the basal turn of the 6-month-old *Tprn*-null mice. The hair cell loss in the *Tprn*-null mice was likely due to the degeneration of stereociliary bundles. Hair cell loss has been reported to be caused by defects in the development and maintenance of actin-based stereociliary bundles in mice [33,36,37]. Thus, considering our results, we propose that TPRN is required for maintaining and stabilizing stereociliary bundles in hair cells, not for the development of the stereociliary bundles in mice.

Tprn is critical for stereociliary rootlet integrity and actin filament assembly in cochlear hair cells in mice

In inner ear hair cells, stereocilia contain a core of actin filaments associated with actin-binding proteins. The stereociliary rootlets extend down to the tapered region and embed in the cuticular plate, where stereocilia are anchored into the actin-rich filamentous meshwork. As observed by electron microscopy, stereociliary rootlets are electron-dense actin skeletal structures at the core of stereociliary bundles in cochlear hair cells. The dense structure of actin filaments in the stereociliary rootlets is important for maintaining stereocilia durability and offers rigidity to stereocilia in mice.

Given the severely disrupted stereociliary bundles at the tapered region in the *Tprn*-null mice, we further examined the stereocilia, especially the actin skeletal structure of the stereociliary rootlets. In the WT mice, each stereocilium is supported by an array of parallel actin filaments [38]. Some actin filaments are packed more densely than others and form a stereociliary rootlet, which is a straight and densely packed central actin-based cytoskeletal structure [4]. During mechanical stimulation, the steady actin structures of stereociliary rootlets pivot around the tapered region and revert to the original straight position [39,40]. Stereociliary rootlets are important for stereocilium stiffness and durability during normal deflection [40]. However, in the *Tprn*-null mice, the disrupted stereociliary rootlets displayed hollow structures surrounded by loose peripheral actin filament rings. This observation indicated that some actin filaments with actin-binding proteins were lost or reduced in number in these stereocilia. In the *Tprn*-null mice, the stereocilia may not return to their original positions after bending. In this case, the cochlear hair cell stereocilia degenerate. These results demonstrated that TPRN loss disrupts the actin-based cytoskeletal structure of the cochlear hair cell stereocilia, especially the stereociliary rootlets. However, the molecular mechanism of TPRN-dependent actin regulation and TPRN's influence on steady actin structures in the cochlear hair cell stereocilia in mice remain to be explored. Stereocilia consist of actin filaments and several actin-binding proteins [34]. Actin filaments are the cytoskeletal structures responsible for stereociliary morphology, and actin-binding proteins participate in the assembly of actin-based structures and the maintenance of stereociliary stability [41]. Stereocilium malformation is often caused by abnormalities in actin structure or mutations in actin-binding proteins, such as taperin, radixin [24], villin [25], fimbrin [26], XIRP2 [27], and FASCIN2 [27]. Previous studies have demonstrated that actin-binding proteins are concentrated at the tapered region and mainly located at the stereocilium core. TPRN interacts with some actin-related proteins, such as radixin and CLIC5 [15]. These proteins

can work together as a complex that stabilizes linkages between the plasma membrane and actin cytoskeleton at the stereocilium base [15]. Radixin regulates actin dynamics and anchoring to the cell membrane in inner ear hair cells [11]. In the *Tprn*-null mice, disordered localization of radixin was observed, with radixin dispersed on the stereocilium. Through Western blot analysis, we found that the relative level of radixin in the *Tprn*-null mice was significantly decreased with respect to that in the WT mice. We propose that a defect in radixin that results from TPRN loss may contribute to the degenerated stereocilia in the *Tprn*-null mice. These results are consistent with a previous report where an intimate relationship between taperin and radixin was noted [7]. As previously described, actin-binding proteins participate in the assembly and stability of the actin-based cytoskeletal stereocilium core [11,14,15]. We then examined the β-actin expression levels. The findings revealed that the relative β-actin level remarkably declined in the *Tprn*-null mice relative to that in the WT mice. Disrupted β-actin and actin-binding proteins, including TPRN and radixin, likely resulted in the hollow structure at the center of stereociliary rootlets and the loose peripheral ring in the *Tprn*-null mice.

Stereociliary bundles are composed of an actin filament core and several actin-binding protein complexes responsible for the assembly and maintenance of highly organized actin-based structures in inner ear hair cells. Among these protein complexes at the tapered region of the stereocilia, Fam65b forms a circumferential ring-like structure that outlines individual stereocilia. TPRN is inside the ring and forms a protein complex with CLIC5 and radixin near the basal tapered region of stereocilia in cochlear hair cells (Fig. 9E). In the *Tprn*-null mice, TPRN loss may lead to the impaired assembly of actin filaments and the abnormal expression and distribution of radixin; such effects can disrupt the complex of taperin, radixin, and CLIC5. The disrupted complex adversely affects the stability and stiffness of actin-based stereociliary rootlets at the stereocilium base. As a result, the damaged stereociliary rootlets become fragile at the tapered region. The stereociliary bundles further deteriorate, and hearing loss aggravates in the *Tprn*-null mice. Overall, TPRN is critical for stereociliary rootlet integrity and actin filament assembly via a molecular complex with radixin in the hearing process.

Tprn-null mice with a CBA/CaJ background are ideal models of nonsyndromic deafness DFNB79 for hearing research

Animal models are extremely important for determining the roles of deafness genes in the hearing process. The genetic background of mice occasionally affects the phenotypes of the mutant mice generated. Thus, using an animal strain with a pure genetic background is important for hearing research. Establishing traditional knockout animal models is based on the use of embryonic stem cells from 129 and C57BL/6 strain backgrounds, which involve ARHL. In hearing research, ARHL can interfere with the study of hearing phenotypes, especially progressive hearing loss in mouse models [41]. In a previous study, generating *Tprn* knockout mouse models by TALEN is based on the use of C57BL/6 strain backgrounds, which are unsuitable for the study of progressive deafness. CBA/CaJ mice possess a pure genetic background and no ARHL [41]. Of 80 inbred strains, this mouse strain was found ideal for hearing research [18]. The CRISPR/Cas9 technology developed in recent years has enabled the generation of mouse models on a pure CBA/CaJ background. We generated the *Tprn* knockout model in a CBA/CaJ mouse strain, which avoided the influence of an adverse genetic background on hearing-related research.

In the present study, we generated a *Tprn*-null mouse model from the CBA/CaJ mouse line. In humans, the hearing loss caused by *TPRN* mutation is progressive and becomes profound by young adulthood. In a report by Li *et al*., two Dutch siblings were diagnosed with sensorineural hearing loss at the age of 4 years and 3 months and 2 years and 9 months, which progressed to profound hearing loss by the ages of 15 and 26 years, respectively [13]. ABR testing demonstrated that the hearing thresholds varied from 60 dB to 80 dB by the age of 20 years. In our study, the *Tprn*-null mice began to show hearing loss as early as 1 month of age; this mouse age is equivalent to approximately 5 years in humans. The *Tprn*-null mice developed severe hearing loss with variation between 60 and 80 dB at 6 months of age, equivalent to approximately 15 years in humans. Thus, the progressive hearing loss in *Tprn*-null mice resembles that of human patients with DFNB79 hearing loss. The generated *Tprn*-null mouse provides an ideal mouse model of the progressive hearing loss DFNB79. To date, no cochlea from patients with *TPRN* mutations has been studied histologically. We studied the malformation of hair cell stereociliary bundles and the potential mechanisms of TPRN function in mouse hair cells through the *Tprn*-null mouse model. We further studied the interaction of *Tprn* and *Radixin* and the mechanisms of hereditary hearing loss, especially in stereociliary bundles, to understand the hearing process. Reexpression of *TPRN* in *TPRN*-null hair cells at postnatal ages can prevent morphological defects and repair hair cell damage in human patients with *TPRN* gene mutations. In conclusion, *Tprn*-null mice can be used not only to examine *Tprn* gene function in the development and maturation of the hearing process, but also as a reference for research on hereditary deafness and therapeutic intervention for deafness.

Acknowledgements

This work was supported by grants from the National Basic Research Program of China (973 Program, No. 2014CB541703), the National Natural Science Foundation of China (No. 81670943), and the Natural Science Foundation of Shandong Province (No. ZR2015PC020).

Compliance with ethics guidelines

Yuqin Men, Xiujuan Li, Hailong Tu, Aizhen Zhang, Xiaolong Fu, Zhishuo Wang, Yecheng Jin, Congzhe Hou, Tingting Zhang, Sen Zhang, Yichen Zhou, Boqin Li, Jianfeng Li, Xiaoyang Sun, Haibo Wang, and Jiangang Gao declare that they have no conflict of interest. All institutional and national guidelines for the care and use of laboratory animals were followed.

References

1. Holley MC. Keynote review: The auditory system, hearing loss and potential targets for drug development. Drug Discov Today 2005; 10 (19): 1269–1282
2. Corwin JT, Warchol ME. Auditory hair cells: structure, function, development, and regeneration. Annu Rev Neurosci 1991; 14(1): 301–333
3. Tilney LG, Saunders JC. Actin filaments, stereocilia, and hair cells of the bird cochlea. I. Length, number, width, and distribution of stereocilia of each hair cell are related to the position of the hair cell on the cochlea. J Cell Biol 1983; 96(3): 807–821
4. Furness DN, Mahendrasingam S, Ohashi M, Fettiplace R, Hackney CM. The dimensions and composition of stereociliary rootlets in mammalian cochlear hair cells: comparison between high- and low-frequency cells and evidence for a connection to the lateral membrane. J Neurosci 2008; 28(25): 6342–6353
5. Müller U, Barr-Gillespie PG. New treatment options for hearing loss. Nat Rev Drug Discov 2015; 14(5): 346–365
6. Fettiplace R, Kim KX. The physiology of mechanoelectrical transduction channels in hearing. Physiol Rev 2014; 94(3): 951–986
7. Gagnon LH, Longo-Guess CM, Berryman M, Shin JB, Saylor KW, Yu H, Gillespie PG, Johnson KR. The chloride intracellular channel protein CLIC5 is expressed at high levels in hair cell stereocilia and is essential for normal inner ear function. J Neurosci 2006; 26(40): 10188–10198
8. Goodyear R, Richardson G. Distribution of the 275 kD hair cell antigen and cell surface specialisations on auditory and vestibular hair bundles in the chicken inner ear. J Comp Neurol 1992; 325(2): 243–256
9. Anderson DW, Probst FJ, Belyantseva IA, Fridell RA, Beyer L, Martin DM, Wu D, Kachar B, Friedman TB, Raphael Y, Camper SA. The motor and tail regions of myosin XV are critical for normal structure and function of auditory and vestibular hair cells. Hum Mol Genet 2000; 9(12): 1729–1738
10. Hasson T, Gillespie PG, Garcia JA, MacDonald RB, Zhao Y, Yee AG, Mooseker MS, Corey DP. Unconventional myosins in inner-ear sensory epithelia. J Cell Biol 1997; 137(6): 1287–1307
11. Pataky F, Pironkova R, Hudspeth AJ. Radixin is a constituent of stereocilia in hair cells. Proc Natl Acad Sci USA 2004; 101(8): 2601–2606
12. Bau S, Schracke N, Kränzle M, Wu H, Stähler PF, Hoheisel JD, Beier M, Summerer D. Targeted next-generation sequencing by specific capture of multiple genomic loci using low-volume microfluidic DNA arrays. Anal Bioanal Chem 2009; 393(1): 171–175
13. Li Y, Pohl E, Boulouiz R, Schraders M, Nürnberg G, Charif M, Admiraal RJ, von Ameln S, Baessmann I, Kandil M, Veltman JA, Nürnberg P, Kubisch C, Barakat A, Kremer H, Wollnik B. Mutations in TPRN cause a progressive form of autosomal-recessive nonsyndromic hearing loss. Am J Hum Genet 2010; 86 (3): 479–484
14. Rehman AU, Morell RJ, Belyantseva IA, Khan SY, Boger ET, Shahzad M, Ahmed ZM, Riazuddin S, Khan SN, Riazuddin S, Friedman TB. Targeted capture and next-generation sequencing identifies C9orf75, encoding taperin, as the mutated gene in nonsyndromic deafness DFNB79. Am J Hum Genet 2010; 86(3): 378–388
15. Salles FT, Andrade LR, Tanda S, Grati M, Plona KL, Gagnon LH, Johnson KR, Kachar B, Berryman MA. CLIC5 stabilizes membrane-actin filament linkages at the base of hair cell stereocilia in a molecular complex with radixin, taperin, and myosin VI. Cytoskeleton (Hoboken) 2014; 71(1): 61–78
16. Zhao B, Wu Z, Müller U. Murine Fam65b forms ring-like structures at the base of stereocilia critical for mechanosensory hair cell function. eLife 2016; 5: e14222
17. Chen M, Wang Q, Zhu GH, Hu P, Zhou Y, Wang T, Lai RS, Xiao ZA, Xie DH. Progressive hearing loss and degeneration of hair cell stereocilia in taperin gene knockout mice. Biochem Biophys Res Commun 2016; 479(4): 703–707
18. Zheng QY, Johnson KR, Erway LC. Assessment of hearing in 80 inbred strains of mice by ABR threshold analyses. Hear Res 1999; 130(1-2): 94–107
19. Fujihara Y, Ikawa M. CRISPR/Cas9-based genome editing in mice by single plasmid injection. Methods Enzymol 2014; 546: 319–336
20. Steigelman KA, Lelli A, Wu X, Gao J, Lin S, Piontek K, Wodarczyk C, Boletta A, Kim H, Qian F, Germino G, Géléoc GS, Holt JR, Zuo J. Polycystin-1 is required for stereocilia structure but not for mechanotransduction in inner ear hair cells. J Neurosci 2011; 31 (34): 12241–12250
21. Men Y, Zhang A, Li H, Zhang T, Jin Y, Li H, Zhang J, Gao J. LKB1 is required for the development and maintenance of stereocilia in inner ear hair cells in mice. PLoS One 2015; 10(8): e0135841
22. Lelli A, Asai Y, Forge A, Holt JR, Géléoc GS. Tonotopic gradient in the developmental acquisition of sensory transduction in outer hair cells of the mouse cochlea. J Neurophysiol 2009; 101(6): 2961–2973
23. Goodyear RJ, Marcotti W, Kros CJ, Richardson GP. Development and properties of stereociliary link types in hair cells of the mouse cochlea. J Comp Neurol 2005; 485(1): 75–85
24. Kitajiri S, Fukumoto K, Hata M, Sasaki H, Katsuno T, Nakagawa T, Ito J, Tsukita S, Tsukita S. Radixin deficiency causes deafness associated with progressive degeneration of cochlear stereocilia. J Cell Biol 2004; 166(4): 559–570

25. Kolb CA, Käser MA, Kopecký J, Zotz G, Riederer M, Pfündel EE. Effects of natural intensities of visible and ultraviolet radiation on epidermal ultraviolet screening and photosynthesis in grape leaves. Plant Physiol 2001; 127(3): 863–875
26. Kopecky D, Hayde M, Prusa AR, Adlassnig KP. Knowledge-based interpretation of toxoplasmosis serology test results including fuzzy temporal concepts—the ToxoNet system. Stud Health Technol Inform 2001; 84(Pt 1): 484–488
27. Francis SP, Krey JF, Krystofiak ES, Cui R, Nanda S, Xu W, Kachar B, Barr-Gillespie PG, Shin JB. A short splice form of Xin-actin binding repeat containing 2 (XIRP2) lacking the Xin repeats is required for maintenance of stereocilia morphology and hearing function. J Neurosci 2015; 35(5): 1999–2014
28. Perrin BJ, Strandjord DM, Narayanan P, Henderson DM, Johnson KR, Ervasti JM. β-Actin and fascin-2 cooperate to maintain stereocilia length. J Neurosci 2013; 33(19): 8114–8121
29. Khan SY, Riazuddin S, Shahzad M, Ahmed N, Zafar AU, Rehman AU, Morell RJ, Griffith AJ, Ahmed ZM, Riazuddin S, Friedman TB. DFNB79: reincarnation of a nonsyndromic deafness locus on chromosome 9q34.3. Eur J Hum Genet 2010; 18(1): 125–129
30. Zheng L, Sekerková G, Vranich K, Tilney LG, Mugnaini E, Bartles JR. The deaf jerker mouse has a mutation in the gene encoding the espin actin-bundling proteins of hair cell stereocilia and lacks espins. Cell 2000; 102(3): 377–385
31. Peng AW, Belyantseva IA, Hsu PD, Friedman TB, Heller S. Twinfilin 2 regulates actin filament lengths in cochlear stereocilia. J Neurosci 2009; 29(48): 15083–15088
32. Sekerková G, Richter CP, Bartles JR. Roles of the espin actin-bundling proteins in the morphogenesis and stabilization of hair cell stereocilia revealed in CBA/CaJ congenic jerker mice. PLoS Genet 2011; 7(3): e1002032
33. Furness DN, Johnson SL, Manor U, Rüttiger L, Tocchetti A, Offenhauser N, Olt J, Goodyear RJ, Vijayakumar S, Dai Y, Hackney CM, Franz C, Di Fiore PP, Masetto S, Jones SM, Knipper M, Holley MC, Richardson GP, Kachar B, Marcotti W. Progressive hearing loss and gradual deterioration of sensory hair bundles in the ears of mice lacking the actin-binding protein Eps8L2. Proc Natl Acad Sci USA 2013; 110(34): 13898–13903
34. Frolenkov GI, Belyantseva IA, Friedman TB, Griffith AJ. Genetic insights into the morphogenesis of inner ear hair cells. Nat Rev Genet 2004; 5(7): 489–498
35. Petit C, Richardson GP. Linking genes underlying deafness to hair-bundle development and function. Nat Neurosci 2009; 12(6): 703–710
36. Drummond MC, Belyantseva IA, Friderici KH, Friedman TB. Actin in hair cells and hearing loss. Hear Res 2012; 288(1-2): 89–99
37. Shahin H, Walsh T, Sobe T, Abu Sa'ed J, Abu Rayan A, Lynch ED, Lee MK, Avraham KB, King MC, Kanaan M. Mutations in a novel isoform of TRIOBP that encodes a filamentous-actin binding protein are responsible for DFNB28 recessive nonsyndromic hearing loss. Am J Hum Genet 2006; 78(1): 144–152
38. Tilney LG, Jaffe LA. Actin, microvilli, and the fertilization cone of sea urchin eggs. J Cell Biol 1980; 87(3): 771–782
39. Kitajiri S, Sakamoto T, Belyantseva IA, Goodyear RJ, Stepanyan R, Fujiwara I, Bird JE, Riazuddin S, Riazuddin S, Ahmed ZM, Hinshaw JE, Sellers J, Bartles JR, Hammer JA 3rd, Richardson GP, Griffith AJ, Frolenkov GI, Friedman TB. Actin-bundling protein TRIOBP forms resilient rootlets of hair cell stereocilia essential for hearing. Cell 2010; 141(5): 786–798
40. Boutet de Monvel J, Petit C. Wrapping up stereocilia rootlets. Cell 2010; 141(5): 748–750
41. Pollard TD, Borisy GG. Cellular motility driven by assembly and disassembly of actin filaments. Cell 2003; 112(4): 453–465
42. Zheng QY, Tong YC, Alagramam KN, Yu H. Tympanometry assessment of 61 inbred strains of mice. Hear Res 2007; 231(1-2): 23–31